

Cosmic Strings Collision in Cosmological Backgrounds

Hassan Firouzjahi^{1,*}, Salomeh Khoeini-Moghaddam^{1,2,†} and Shahram Khosravi^{2,3‡}

¹ *School of Physics, Institute for Research in Fundamental Sciences (IPM),*

P. O. Box 19395-5531, Tehran, Iran

² *Department of Physics, Faculty of Science,*

Tarbiat Mo'alleem university, Tehran, Iran and

³*School of Astronomy, Institute for Research in Fundamental Sciences (IPM), Tehran, Iran*

(Dated: February 14, 2022)

Abstract

The collisions of cosmic strings loops and the dynamics of junctions formations in expanding backgrounds are studied. The key parameter controlling the dynamics of junctions formation, the cosmic strings zipping and unzipping is the relative size of the loops compared to the Hubble expansion rate at the time of collision. We study analytically and numerically these processes for large super-horizon size loops, for small sub-horizon size loops as well as for loops with the radii comparable to the Hubble expansion rate at the time of collision.

PACS numbers:

*Electronic address: firouz(AT)ipm.ir

†Electronic address: skhoeini(AT)tmu.ac.ir

‡Electronic address: khosravi(AT)ipm.ir

I. INTRODUCTION

In models of brane inflation cosmic strings are copiously produced [1, 2], for reviews see e.g. [3–7]. These cosmic superstrings are in the forms of fundamental strings (F-strings), D1-branes (D-strings) or the bound states of p F-strings and q D-strings, the (p, q) strings. When two (p, q) cosmic superstrings collide junctions are formed due to charge conservation. This is in contrast to the collision of conventional gauge strings where upon collision they exchange partners and intercommute with the probability close to unity. Therefore one may consider the junction formation as a novel feature of a network of cosmic superstrings which may prove crucial in cosmic superstrings detection in cosmological observations. Networks of cosmic strings with junctions have interesting physical properties, such as the formation of multiple images [8, 9] and non-trivial gravitational wave emission [10, 11]. Different theoretical aspects of (p, q) string construction were studied in [12–17] while the cosmological evolution of a string network with junctions has been investigated in [18].

In a recent paper [19] the collision of two loops of cosmic strings in a flat background was studied. It was found that with appropriate initial conditions determined by the angle of collision, the colliding loops velocities and the loops relative tensions, junctions can form. However, after the junction is formed it can not grow indefinitely and after some time the junction start to unzip and the colliding loops disentangle and pass by from each other. The junctions' zipping and unzipping are interesting and yet non-trivial dynamical properties. These phenomena becomes more significant in the light of cosmic strings simulation by Urrestilla and Vilenkin [20]. In their model, the cosmic strings are two types of U(1) gauge strings with interactions between them. Due to the interaction, the strings cannot exchange partners and a bound state will form if the strings are not moving too fast. It was shown that the length and the distribution of the string network are dominated by the original strings and there is a negligible contribution to the string network length and population from the bound states strings. This can be understood based on the following two reasons. Firstly, the junctions may not form if the colliding strings are moving very fast so they can simply pass through each other [21–27]. Secondly and more interestingly, if the junctions are formed, they start to unzip during the evolution.

Our aim here is to generalize the results of [19] to the case of cosmic strings loops collision in cosmological backgrounds, i.e. the radiation and the matter dominated era. As we shall

see in sections III and IV, the size of the loops compared to the Hubble radius at the time of collision plays a significant role in junctions evolutions and cosmic strings zipping and unzipping.

The paper is organized as follows. In section II we present our set up and provide the formalism of junction formation for arbitrary cosmic strings loops colliding in cosmological backgrounds. This is a generalization of [22] and [28] where they presented the formalism of cosmic strings collision in the flat background. In section III we concentrate to the example of two identical loops in cosmological backgrounds. After setting the background equations for the loops profiles, we present the equations governing the dynamics of the junctions. For the case of very large loops (super-horizon size loops) and very small loops (sub-horizon size loops) we are able to present some analytical results. In section IV we present our full numerical results for different loop configurations. The conclusion is given in section V

II. LOOPS COLLISION IN AN EXPANDING UNIVERSE

Here we present the formalism of junction formation for arbitrary cosmic strings loops colliding in a cosmological background. In section III we employ the results obtained in this section to the particular example of two identical loops at collision in cosmological backgrounds. The formalism of cosmic strings collision in a flat background was studied in [22] and [28].

Our cosmological background is the standard FRW metric

$$ds^2 = a^2(\tau)(d\tau^2 - d\mathbf{x}^2), \quad (1)$$

where τ is the conformal time related to the cosmic time t via $dt = ad\tau$, $a(\tau)$ is the scale factor and we assume that the background space-time has no spatial curvature. Our cosmological background is either radiation dominated (RD) or matter dominated (MD).

Suppose X_i^μ represents the profile of the i -th cosmic string in the target space-time. As usual, we can go to the temporal gauge where the time on the string world-sheet is the same as the conformal time, $X^0 = \tau$, and $X_i^\mu = (\tau, \mathbf{x}_i)$. Denoting the other coordinate of the world-sheet parameterization by σ , the gauge condition

$$\dot{\mathbf{x}}_i \cdot \mathbf{x}'_i = 0, \quad (2)$$

holds where the \cdot and the prime indicate the derivatives with respect to τ and σ respectively.

A schematic view of two loops of cosmic strings in collision is shown in **Fig. 1**. After collision, there are four junctions and eight kinks. The formation of the kinks is a manifestation of the fact that the speed of light is finite and parts of the old strings which did not “feel” the formation of junctions evolve as before. In the following we denote the incoming strings by \mathbf{x}_i where $i = 1, 2$ whereas the newly formed strings are denoted by \mathbf{y}_a where $a = 1, 2, 3$. The junctions and the kinks on each string are described by $\sigma_a = s_a(\tau)$ and $\sigma_i = \omega_i(\tau)$ respectively.

As mentioned in [19, 28] one complexity of dealing with loops in collision is the orientation of the σ_i coordinate at junctions. We follow the prescription of [28] and use the sign parameterization for δ_a^J according to which δ_a^J can take values ± 1 . If the value of σ_a of a particular string increases(decreases) towards the junction J , we assign $\delta_a^J = +1(\delta_a^J = -1)$. With this prescription, the two ends of a piece of string ending in two neighboring junctions have opposite δ parameters. The arrows in **Fig. 1** indicate this prescription. Since it is important for the later analysis, we now give the values of δ_a^J at each junction:

$$A : \begin{vmatrix} \delta_1 = +1 \\ \delta_2 = -1 \\ \delta_3 = -1 \end{vmatrix} \quad B : \begin{vmatrix} \delta_1 = -1 \\ \delta_2 = +1 \\ \delta_3 = +1 \end{vmatrix} \quad C : \begin{vmatrix} \delta_1 = -1 \\ \delta_2 = +1 \\ \delta_3 = +1 \end{vmatrix} \quad D : \begin{vmatrix} \delta_1 = +1 \\ \delta_2 = -1 \\ \delta_3 = -1 \end{vmatrix} \quad (3)$$

Equipped with the δ -prescription, the action for the system of two loops in collision is

$$\begin{aligned} \mathbf{S} = & - \sum_J \sum_{i=1}^2 \mu_i \int d\tau d\sigma_i a^2(\tau) \sqrt{(1 - \dot{\mathbf{y}}_i^2)} \mathbf{y}_i'^2 \theta(\delta_i^J(s_i^J(\tau) - \sigma_i)) \theta(\delta_i^J(\sigma_i - \omega_i^J(\tau))) \quad (4) \\ & - \sum_{i=1}^2 \mu_i \int d\tau d\sigma_i a^2(\tau) \sqrt{(1 - \dot{\mathbf{x}}_i^2)} \mathbf{x}_i'^2 \theta(\delta_i^A(\omega_i^A(\tau) - \sigma_i)) \theta(\delta_i^B(\omega_i^B(\tau) - \sigma_i)) \\ & - \sum_{i=1}^2 \mu_i \int d\tau d\sigma_i a^2(\tau) \sqrt{(1 - \dot{\mathbf{x}}_i^2)} \mathbf{x}_i'^2 \theta(\delta_i^C(\omega_i^C(\tau) - \sigma_i)) \theta(\delta_i^D(\omega_i^D(\tau) - \sigma_i)) \\ & - \mu_3 \int d\tau d\sigma_3 a^2(\tau) \sqrt{(1 - \dot{\mathbf{y}}_3^2)} \mathbf{y}_3'^2 \theta(\delta_3^A(s_3^A(\tau) - \sigma_3)) \theta(\delta_3^C(s_3^C(\tau) - \sigma_3)) \\ & - \mu_3 \int d\tau d\sigma_3 a^2(\tau) \sqrt{(1 - \dot{\mathbf{y}}_3^2)} \mathbf{y}_3'^2 \theta(\delta_3^B(s_3^B(\tau) - \sigma_3)) \theta(\delta_3^D(s_3^D(\tau) - \sigma_3)) \\ & + \sum_J \sum_{a=1}^3 \int d\tau a^2(\tau) \mathbf{f}_a^J \cdot [\mathbf{y}_a(s_a^J(\tau), \tau) - \bar{\mathbf{y}}^J(\tau)] \\ & + \sum_J \sum_{i=1}^2 \int d\tau a^2(\tau) \mathbf{k}_i^J \cdot [\mathbf{x}_i(\omega_i^J(\tau), \tau) - \mathbf{y}_i(\omega_i^J(\tau), \tau)] \end{aligned}$$

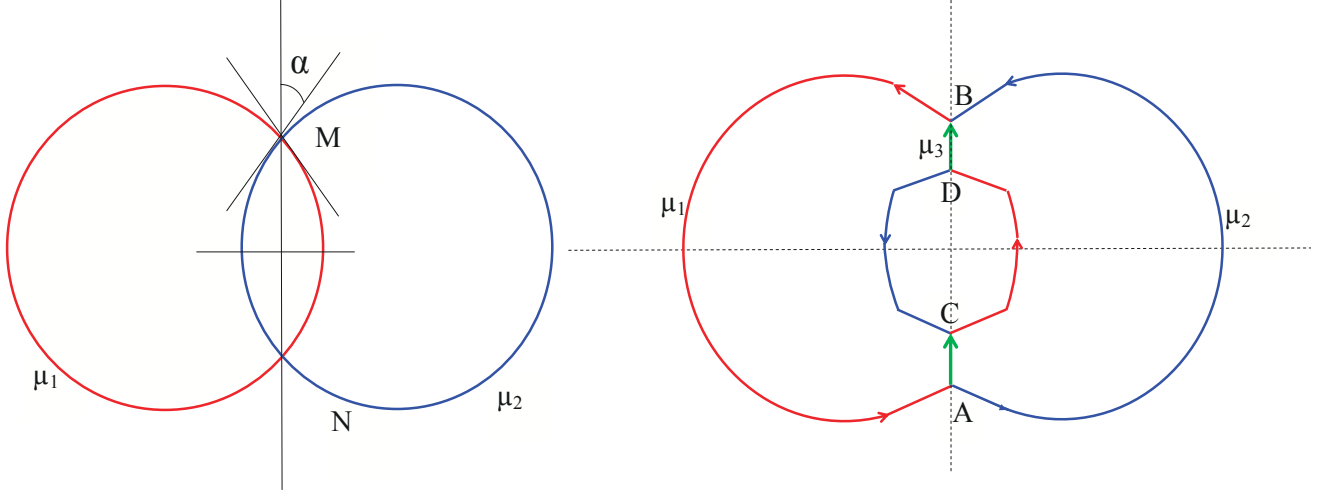


FIG. 1: A schematic view of the loops at the time of collision(left) and after collision (right). The arrows in the right figure indicate the directions in which the σ_i coordinate increases. We use the convention that on a loop σ_i runs counter clockwise. There are four junctions and eight kinks in total.

where J represents the junctions A, B, C and D collectively. Here \mathbf{f}_a^J and \mathbf{k}_i^J are Lagrange multipliers which enforce that at the kinks the newly formed strings and the old strings meet, $\mathbf{x}_i(\omega_i^J(\tau), \tau) = \mathbf{y}_i(\omega_i^J(\tau), \tau)$ and on the junctions the three newly formed strings join together $\mathbf{y}_a(s_a^J(\tau), \tau) = \bar{\mathbf{y}}^J(\tau)$ where $\bar{\mathbf{y}}^J(\tau)$ represents the position of the junction J in target space. As described above, in our convention δ_i^J is +1 if σ increases towards the junction and -1 in the opposite case.

Varying the action with respect to $\mathbf{f}_a^J, \mathbf{k}_a^J$ and $\bar{\mathbf{y}}_a^J$, respectively, results in

$$\mathbf{y}_a(s_a^J(\tau), \tau) = \bar{\mathbf{y}}^J(\tau) \quad (5)$$

$$\mathbf{x}_i(\omega_i^J(\tau), \tau) = \mathbf{y}_i(\omega_i^J(\tau), \tau) \quad (6)$$

$$\sum_a \mathbf{f}_a^J = 0. \quad (7)$$

Varying the action with respect to \mathbf{x}_i results in the following standard equations [29] for the segments of old strings extended between two nearby kinks which are not influenced by the junctions formations

$$\frac{\partial}{\partial \tau}(\dot{\mathbf{x}}_i \epsilon_{\mathbf{x}_i}) + 2 \frac{\dot{a}}{a} \dot{\mathbf{x}}_i \epsilon_{\mathbf{x}_i} = \frac{\partial}{\partial \sigma} \left(\frac{\mathbf{x}'_i}{\epsilon_{\mathbf{x}_i}} \right), \quad (8)$$

whereas matching the Dirac delta functions gives the following boundary conditions at the kinks $\sigma_i = \omega_i^J(\tau)$

$$\mathbf{k}_i^J = \mu_i \left(\dot{\mathbf{x}}_i \epsilon_{\mathbf{x}_i} \dot{\omega}_i^J \delta_i^J + \frac{\mathbf{x}_i'}{\epsilon_{\mathbf{x}_i}} \delta_i^J \right) \quad , \quad \sigma_i = \omega_i^J(\tau) . \quad (9)$$

Here ϵ_i is defined by [29]

$$\epsilon_i \equiv \sqrt{\frac{\mathbf{x}_i'^2}{1 - \dot{\mathbf{x}}_i^2}} \quad (10)$$

Similarly, varying the action with respect to \mathbf{y}_a results in the following equations for the newly formed strings stretched between a junction and the nearby kink

$$\frac{\partial}{\partial \tau}(\dot{\mathbf{y}}_a \epsilon_{\mathbf{y}_a}) + 2 \frac{\dot{a}}{a} \dot{\mathbf{y}}_a \epsilon_{\mathbf{y}_a} = \frac{\partial}{\partial \sigma} \left(\frac{\mathbf{y}_i'}{\epsilon_{\mathbf{y}_i}} \right) . \quad (11)$$

Now there are Dirac delta functions at the junctions $\sigma_a = s_a^J(\tau)$ and the kinks (for strings 1 and 2) $\sigma_i = \omega_i^J$ which result in the following boundary conditions

$$\mathbf{k}_i^J = \mu_i \left(\dot{\mathbf{y}}_i \epsilon_{\mathbf{y}_i} \dot{\omega}_i^J \delta_i^J + \frac{\mathbf{y}_i'}{\epsilon_{\mathbf{y}_i}} \delta_i^J \right) \quad , \quad \sigma_i = \omega_i^J(\tau) \quad (12)$$

$$\mathbf{f}_a^J = \mu_a \left(\dot{\mathbf{y}}_a \epsilon_{\mathbf{y}_a} \dot{s}_a^J \delta_a^J + \frac{\mathbf{y}_a'}{\epsilon_{\mathbf{y}_a}} \delta_a^J \right) \quad , \quad \sigma_a = s_a^J(\tau) . \quad (13)$$

Combining Eqs (7) and (13) result in

$$\sum_a \mu_a \delta_a^J \left(\dot{\mathbf{y}}_a \epsilon_{\mathbf{y}_a} \dot{s}_a^J + \frac{\mathbf{y}_a'}{\epsilon_{\mathbf{y}_a}} \right) = 0 . \quad (14)$$

Eliminating \mathbf{k}_i^J from Eqs. (9) and (12), and using the gauge condition (2), it is easy to show that

$$\epsilon_{\mathbf{x}_i} = \epsilon_{\mathbf{y}_i} = \epsilon_i \quad (15)$$

$$\delta_i^J \dot{\omega}_i^J \epsilon_i = -1 \quad (16)$$

The solutions of the loops in cosmological backgrounds can not be expressed in terms of the the usual right- and left-movers. However, one can define the right- and left-momenta \mathbf{p}_a^\pm as

$$\begin{aligned} \mathbf{p}_{\mathbf{y}_a}^{\pm J} &= \frac{\mathbf{y}_a'}{\epsilon_a} \pm \delta_a^J \dot{\mathbf{y}}_a \\ \mathbf{p}_{\mathbf{x}_i}^{\pm J} &= \frac{\mathbf{x}_i'}{\epsilon_i} \pm \delta_i^J \dot{\mathbf{x}}_i \end{aligned} \quad (17)$$

with $\mathbf{p}_a^{\pm 2} = 1$. Starting with the time derivative of (5)

$$\mathbf{x}'\dot{\omega}_i^J + \dot{\mathbf{x}}_i = \mathbf{y}'\dot{\omega}_i^J + \dot{\mathbf{y}}_i, \quad (18)$$

one can show that $\mathbf{p}_{\mathbf{y}_i}^{-J} = \mathbf{p}_{\mathbf{x}_i}^{-J}$. This is the key formula which relates the unknown quantities $\mathbf{p}_{\mathbf{y}_i}^{-J}$ for the newly formed strings to the known quantities $\mathbf{p}_{\mathbf{x}_i}^{-J}$ from the old strings.

Starting with the time-derivative of Eq. (5) combined with Eq. (14) one obtains an equation for $\mathbf{p}_{\mathbf{y}_a}^+$ in terms of $\mathbf{p}_{\mathbf{y}_b}^-$

$$\delta_a^J(1 + \delta_a^J \epsilon_a \dot{s}_a^J) \mathbf{p}_{\mathbf{y}_a}^+ = \delta_a^J(1 - \delta_a^J \epsilon_a \dot{s}_a^J) \mathbf{p}_{\mathbf{y}_a}^- - \frac{2}{\bar{\mu}} \sum_b \mu_b \delta_b^J(1 - \delta_b^J \epsilon_b \dot{s}_b^J) \mathbf{p}_{\mathbf{y}_b}^-. \quad (19)$$

Imposing the condition $\mathbf{p}_a^{\pm 2} = 1$ one obtains

$$q_a - q_a \sum_b \bar{\mu}_b q_b c_{ab} + \sum_{bc} \bar{\mu}_b \bar{\mu}_c q_b q_c c_{bc} - 1 = 0 \quad (20)$$

where $\bar{\mu}_a \equiv \mu_a/\bar{\mu}$, $\bar{\mu} \equiv \sum_a \mu_a$, $q_a^J \equiv 1 - \delta_a^J \epsilon_a \dot{s}_a^J$ and $c_{ab} \equiv \delta_a^J \delta_b^J \mathbf{p}_{\mathbf{y}_a}^- \cdot \mathbf{p}_{\mathbf{y}_b}^-$.

Now we provide an equation for the energy conversation at the junction. For this purpose, multiplying Eq (20) by $\bar{\mu}_a$ and summing over a results in

$$\sum_a \bar{\mu}_a q_a - \sum_{ab} \bar{\mu}_a \bar{\mu}_b c_{ab} + \sum_{abc} \bar{\mu}_a \bar{\mu}_b \bar{\mu}_c q_b q_c c_{ab} - 1 = 0 \quad (21)$$

However, with the reshuffling of the indices, one can easily check that the second and the third term above cancel out and one obtains

$$\sum_a \bar{\mu}_a q_a = 1 \quad (22)$$

or

$$\sum_a \delta_a^J \mu_a \epsilon_a \dot{s}_a = 0. \quad (23)$$

This is a generalization of the case of strings in flat background studied in [22] corresponding to $\epsilon_a = 0$.

Defining $\hat{c}_{ab} = 1 - c_{ab}$ and using the energy conservation one can check that Eq. (20) results in

$$q_a \sum_b \bar{\mu}_b \hat{c}_{ab} q_b = \sum_{bc} \bar{\mu}_b \bar{\mu}_c \hat{c}_{bc} q_b q_c \quad (24)$$

Writing explicitly, and using (23), yields

$$q_1(1 - 2\bar{\mu}_1)(\bar{\mu}_2 q_2 \hat{c}_{12} + \bar{\mu}_3 q_3 \hat{c}_{13}) = 2\bar{\mu}_2 \bar{\mu}_3 q_2 q_3 \hat{c}_{23} \quad (25)$$

$$q_2(1 - 2\bar{\mu}_2)(\bar{\mu}_1 q_1 \hat{c}_{12} + \bar{\mu}_3 q_3 \hat{c}_{23}) = 2\bar{\mu}_1 \bar{\mu}_3 q_1 q_3 \hat{c}_{13} \quad (26)$$

$$q_3(1 - 2\bar{\mu}_3)(\bar{\mu}_2 q_2 \hat{c}_{23} + \bar{\mu}_1 q_1 \hat{c}_{13}) = 2\bar{\mu}_2 \bar{\mu}_1 q_2 q_1 \hat{c}_{12} . \quad (27)$$

Eliminating q_3 and q_2 from the first two equations above and plugging in (23) results in our main formula of interest

$$1 - \delta_1^J \epsilon_1 \dot{s}_1^J = \frac{\bar{\mu} M_1 \hat{c}_{23}}{\mu_1 [M_1 \hat{c}_{23} + M_2 \hat{c}_{13} + M_3 \hat{c}_{12}]}, \quad (28)$$

where $M_1 \equiv \mu_1^2 - (\mu_2 - \mu_3)^2$ with a similar definition for M_2 and M_3 . One can also obtain a similar equation for $\dot{s}_{2,3}$ with an appropriate permutation of the indices. This set of equations for \dot{s}_a^J is our starting point to study the evolutions of junctions.

III. JUNCTION EVOLUTIONS

In previous section we have presented the general formalism of cosmic strings loops collision in a cosmological background. Here we specialize to the example of two identical loops at collision in a cosmological background where the analysis can be handled somewhat analytically.

Before dealing with the loops in collision, here we summarize the background solutions for a loop in expanding background. Suppose the collision happens at the time $\tau = \tau_0$. One can check that the cosmic time t and the conformal time τ are related by $t = \tau^{n+1}/\tau_0^n(n+1)$ where we have considered a power law expansion for the scale factor $a(\tau) = (\tau/\tau_0)^n$. For a radiation and matter dominated universe, $n = 1, 2$ respectively. In this convention, the scale factor at the time of collision is equal to unity. Also, calculating the Hubble expansion rate, $H = da/a dt$, one can check that the Hubble expansion rate at the time of collision is $H_0 = n/\tau_0$.

Consider a loop extended in $x - y$ plane moving relativistically in z direction. We choose the following ansatz for the loop configuration

$$\mathbf{x} = \begin{pmatrix} f(\tau) \cos \frac{\sigma}{R_0} \\ f(\tau) \sin \frac{\sigma}{R_0} \\ z(\tau) \end{pmatrix}. \quad (29)$$

In this picture, $R(\tau) \equiv a(\tau)f(\tau)$ is the physical radius of the loop and $R_0 = f(\tau_0)$ represents the size of the loop at the time of collision.

The independent equations of motions are

$$F'' + \frac{2n}{x}F'(1 - v^2 - F'^2) + (1 - v^2 - F'^2)F^{-1} = 0 \quad (30)$$

$$v' + \frac{2n}{x}v(1 - v^2 - F'^2) = 0. \quad (31)$$

Here the loop center of mass velocity is defined by $v = \dot{z}(\tau)$. For the ease of the numerical investigations, we introduced the dimensionless time variable $x \equiv \tau/\tau_0$ and $F(x) \equiv f(\tau)/\tau_0$. Also the prime here and below represents derivatives with respect to the dimensionless time x .

This definition leads to $F = fH_0/n$ which has a simple physical interpretation as follows. In our convention $a(x) = x^n$, so at the time of collision, corresponding to $x = 1$, $a = 1$. The physical radius of the loop at the time of collision therefore is $R_0 = f(x = 1)$. Therefore, the initial condition $F(x = 1) = f(x = 1)H_0/n$ is a measure of the physical radius of the loop compared to the Hubble radius at the time of collision. For Loops of super-horizon size at the time of collision $F(x = 1) > 1$, whereas for small sub-horizon sized loops at the time of collision $F(x = 1) < 1$. In the following, to simplify the notation we set $F(x = 1) \equiv F_1$.

In general it is not easy to find analytical solutions for the set of equations (30) and (31). We solve this equation numerically. Our goal is to calculate \hat{c}_{ab} for the loop with ansatz (29) and then obtain the evolution of junctions \dot{s}_a^J . However, one may get some useful analytical information in some certain limits. These include very large super-horizon size loops at the time of collision ($F_1 \gg 1$) and small sub-horizon size loops ($F_1 \ll 1$).

The collisions of loops in Minkowski background was studied in [19]. Here we generalize that study to the case of strings loops collision in an expanding background. In order to simplify the analysis, we consider the symmetric case where the two incoming loops have equal tension and physical radius at the time of collision. We assume that the loops are extended in $x - y$ plane and are moving along the z -direction with velocity $\pm v$. A schematic view of this example is given in **Fig. 1**. By symmetry the newly formed string 3 will be static extended either along x or y directions. Whether it is a x -link or a y -link junction depends on the angle of collision α [22]. For small enough angle of collision it is a y -link while for a large enough angle of collision it would be an x -link junction. To be specific, we consider a y -link junction where the string 3 is extended along the y -direction.

The profiles of the colliding loops are given by

$$\mathbf{x}_i = \begin{pmatrix} \mp b + f(\tau) \cos \frac{\sigma_i}{R_0} \\ f(\tau) \sin \frac{\sigma_i}{R_0} \\ \pm z(\tau) \end{pmatrix} \quad (32)$$

where for $i=1$ ($i=2$) we choose upper sign (lower sign). Here $2b$ is the impact factor.

From the continuity of the left moving momenta one has $\mathbf{p}_{\mathbf{y}_i}^{-J} = \mathbf{p}_{\mathbf{x}_i}^{-J}$ which can be served to find $\mathbf{p}_{\mathbf{y}_i}^{-J}$. From (17) we have

$$\mathbf{p}_{\mathbf{y}_i}^{-J} = \mathbf{p}_{\mathbf{x}_i}^{-J} = \begin{pmatrix} -\sqrt{1 - F'^2 - v^2} \sin \frac{\sigma_i}{R_0} - \delta_i^J F' \cos \frac{\sigma_i}{R_0} \\ \sqrt{1 - F'^2 - v^2} \cos \frac{\sigma_i}{R_0} - \delta_i^J F' \sin \frac{\sigma_i}{R_0} \\ \mp \delta_i^J v(\tau) \end{pmatrix} \quad (33)$$

Using $\hat{c}_{ab}^J \equiv 1 - \delta_a^J \delta_b^J \mathbf{p}_{\mathbf{y}_a}^{-J} \cdot \mathbf{p}_{\mathbf{y}_b}^{-J}$ at each junction and the fact that $\delta_1^J = -\delta_2^J = -\delta_3^J$, one obtains

$$\hat{c}_{11}^J = \hat{c}_{22}^J = \hat{c}_{33}^J = 0 \quad (34)$$

$$\hat{c}_{12}^J = 1 + v^2 - (1 - 2F'^2 - v^2) \cos 2S_1^J + 2\delta_1^J F' \sqrt{1 - F'^2 - v^2} \sin 2S_1^J \quad (35)$$

$$\hat{c}_{13}^J = 1 + \sqrt{1 - F'^2 - v^2} \cos S_1^J - \delta_1^J F' \sin S_1^J \quad (36)$$

$$\hat{c}_{23}^J = 1 - \sqrt{1 - F'^2 - v^2} \cos S_2^J - \delta_1^J F' \sin S_2^J \quad (37)$$

$$\hat{c}_{23}^J + \hat{c}_{13}^J = 2 + 2\sqrt{1 - F'^2 - v^2} \cos S_1^J - 2\delta_1^J F' \sin S_1^J \quad (38)$$

Here and below, to simplify the notation the definition $S_a^J \equiv s_a^J/R_0$ is introduced. We note that S_a^J is dimensionless which is more suitable for numerical analysis. To obtain Eqs. (35-37) we note that due to symmetry in problem, one has $S_1'^J = -S_2'^J$ at each junction J . On the other hand, one also observes that $S_1^B(x=1) + S_2^B(x=1) = \pi$ and $S_1^A(x=1) + S_2^A(x=1) = 3\pi$ which was used to simplify the final results in Eqs. (35-37).

Plugging \hat{c}_{ab} in our master equation (28), the evolution of the junction is given by

$$S_3'^J = \frac{\delta_3^J (\kappa - 1)(\hat{c}_{13} + \hat{c}_{23}) - \kappa \hat{c}_{12}}{F_1 (\kappa - 1)(\hat{c}_{13} + \hat{c}_{23}) + \hat{c}_{12}}, \quad (39)$$

where the dimensionless parameter κ is given by the ratio of the tensions $\kappa \equiv 2\mu_1/\mu_3$.

Also from the energy conservation Eq. (23) one has

$$S_1'^J = \frac{F_1}{\kappa F} \sqrt{1 - F'^2 - v^2} S_3'^J. \quad (40)$$

Equations (39) and (40) jointly can be used to solve for $S_3'^J$. Due to symmetries involved in the problem, we only need to find the evolution of junctions B and D and the evolutions of junctions A and C are mirror images of junctions B and D . We note that the conditions for the junction formation is that the string 3 stretching between junctions B and D to be created. This requires that its length to increase initially with time: $S_3' > 0$ where $S_3 \equiv S_3^B - S_3^D$ measures the length of string BD . As we shall see in our numerical results, usually this is translated into $S_3^{B'} > 0$ and $S_3^{D'} < 0$. However, in some very fine-tuned situations one can also find examples where $S_3^{B'} > 0$ and $S_3^{D'} > 0$ such that $S_3' > 0$ is still satisfied.

As explained in [19], after the junction formation, the entangled loops start to unzip. The onset of unzipping at junction J happens when $S_3'^J$ vanishes and changes its sign. As we shall see later, the unzipping times for junctions B and D are not equal. Since we are mainly interested in the evolution of the newly formed string BD , we define the onset of unzipping for string BD when S_3 reaches a maximum and $S_3' = 0$. After that the length of string BD reduces with time. Sometime after unzipping, the loops disentangle from each other and pass by in opposite directions. The time of loops disentanglement happens when the junctions B and D meet corresponding to $S_3 = 0$. However, we also encounter examples where the loops shrink to zero before they disentangle from each other.

As explained above, the onset of unzipping at junction J is determined when $S_3'^J = 0$. Here we show that the denominator in Eq. (39) is always positive so the sign of $S_3'^J$ is controlled by the numerator of the above expressions. To see that note that $-\sqrt{p^2 + q^2} \leq p \cos \theta + q \sin \theta \leq \sqrt{p^2 + q^2}$ for real numbers p and q and arbitrary angle θ . Using these inequalities, one can easily check that $\hat{c}_{12} \geq 2v^2$ and $\hat{c}_{13} + \hat{c}_{23} \geq 2(1 - \sqrt{1 - v^2})$. On the other hand, as described in [22], one also requires that $2\mu_1 > \mu_3$ for the junction formation to be allowed kinematically. In conclusion the denominator in $S_3'^J$ expression is always positive and the sign of $S_3'^J$ evolution is determined by the numerator of the above expressions. This plays important rules in determining the junctions unzipping times in the following discussions.

As explained before, our goal is to solve the background loop equations (30) and (31) and use the resulting values of $F(x)$ and $v(x)$ in \hat{c}_{ab} expressions to find the junctions evolutions from Eq. (39). This procedure can be done only numerically because both $F(x)$ and $v(x)$ can not be found analytically in general. Before presenting our full numerical analysis, we

consider two different limits where some analytical insights can be obtained for the junctions evolutions.

A. Large super-horizon size loops

Here we consider the limit where the colliding loops are much larger than the Hubble radius at the time of collision, $F_1 \gg 1$. For the super-horizon size loops, one expect that they are conformally stretched as the universe expands, $R(\tau) \propto a(\tau)$, where F' and F'' are small compared to unity. We will demonstrate this in our numerical analysis. Due to damping effects from the expanding background, the super-horizon loops become non-relativistic and $v \ll 1$. In this approximation, one can easily solve the background equations (30) and (31). Denoting $F = F_1 + \Delta$ where Δ represents the small evolution of F , one obtains

$$\Delta'' + \frac{2}{x}\Delta' + \frac{1}{F_1} \simeq 0,$$

which after neglecting the sub-dominant term, results in

$$\Delta \simeq -\frac{x^2}{2(1+2n)F_1} \quad , \quad F' \simeq -\frac{x}{(1+2n)F_1}. \quad (41)$$

As the universe expands, the loop reenter the horizon in its subsequent evolutions. This can be approximated when $\Delta \simeq -F_1$ which results in the time of the loop horizon reentry x_*

$$x_* \simeq \sqrt{2(1+2n)F_1}. \quad (42)$$

Our full numerical analysis, as we shall see in next section, verify that this is indeed a good approximation. From this expression for x_* we see that with similar initial conditions, it takes longer for the loops to reenter the horizon in a matter dominated era as compared to the radiation dominated era.

As the super-horizon size loops stretches conformally, its center of mass velocity reduces rapidly. For time smaller than x_* one can find an approximate solution for $v(x)$. Neglecting the terms containing v^2 and F'^2 in Eq. (31) one obtains $v' + 2n v/x \simeq 0$ which easily can be solved to give

$$v(x) \simeq \frac{v_1}{x^{2n}}, \quad (43)$$

where v_1 is the value of $v(x)$ at the time of collision, $v_1 \equiv v(x = 1)$. As explained above, we see that the loop central mass velocity reduces rapidly with time. We also see that for the matter dominated background with $n = 2$, the loss of velocity is more pronounced as compared to the radiation dominated background with $n = 1$.

For the super-horizon size loops and keeping only terms up to F' in \hat{c}_{ab} and neglecting F'^2 and v^2 as explained above, one obtains

$$\hat{c}_{12} \simeq 1 - \cos 2S_1^J + 2\delta_1^J F' \sin 2S_1^J \quad , \quad \hat{c}_{13} + \hat{c}_{23} \simeq 2 + 2 \cos S_1^J - 2\delta_1^J F' \sin S_1^J$$

Plugging these into $S_3'^J$ expression results in

$$S_3'^J \simeq \frac{\delta_3^J (1 + \cos S_1^J) (\kappa \cos S_1^J - 1) - \delta_1^J F' \sin S_1^J (\kappa - 1 + 2\kappa \cos S_1^J)}{F_1 (1 + \cos S_1^J) (-\cos S_1^J + \kappa) - \delta_1^J F' \sin S_1^J (\kappa - 1 - 2 \cos S_1^J)} . \quad (44)$$

At the time of collision, one can neglect the terms containing F' in above expression and for small x one obtains

$$S_3'^B(x \simeq 1) \simeq \frac{\delta_3^J}{F_1} \frac{\kappa \cos S_1^J - 1}{\kappa - \cos S_1^J} . \quad (45)$$

For the junction to form we need $S_3'^B(x = 1) > 0$. With $S_1^B(x = 1) = \alpha$, the condition for junction formation is translated into

$$0 \leq \alpha \leq \alpha_c \quad , \quad \alpha_c = \arccos(\kappa^{-1}) . \quad (46)$$

Interestingly, this is identical to the bound obtained in [23] for straight strings in collision at the small velocity approximation. This is expected, since the super-horizon size loops can be locally well approximated by the straight strings. Our full numerical analysis, presented in next section, indeed show that the bound on α_c given by the above equation works very accurately for the large loops.

As time goes by, the terms containing F' in Eq. (44) becomes important. We note that the denominator in Eq. (44) is positive so the sign of S_3^J evolution is determined by the numerator of Eq. (44). Consider junction B for example. For the junction B to unzip, S_3^B should slow down, requiring that the term containing F' in numerator of Eq. (44) gives a negative contribution. With $\delta_1^B = -1$ and $F' < 0$ the F' correction in numerator of Eq. (44) indeed contributes negatively. This indicates that as time goes by, the rate of evolution of S_3^B slows down until $S_3'^B = 0$ when the junction B starts to unzip. Similar argument applies to junction D too.

B. Small sub-horizon size loops

Now we consider the limit where the colliding loops are much smaller than the Hubble radius at the time of collision, $F_1 \ll 1$. In this limit, the damping terms in Eqs. (30) can be neglected [29] and the loop evolution is the same as in the flat background. In this limit v is nearly constant and the loop has a simple periodic profile

$$F(x) \simeq F_1 \cos \left(\frac{x-1}{\gamma F_1} \right), \quad (47)$$

where $\gamma = 1/\sqrt{1-v^2}$ is the Lorentz factor. To simplify the analysis, here we chose the initial configuration such that $F' = 0$ at the time of collision. Neglecting the effects of expansion, one would expect the criteria for zipping, unzipping and the loops disentanglement would be similar to cosmic strings loops collision in a flat background studied in [19].

Starting from the energy conservation formula (40), one obtains

$$S_1^{B(D)} = \frac{S_3^{B(D)}}{\kappa\gamma} + \alpha. \quad (48)$$

Also calculating \hat{c}_{ab} yields

$$\begin{aligned} \hat{c}_{12} &= 2 - 2\gamma^{-2} \cos^2 \left(S_1^J + \delta_3^J \frac{x-1}{\gamma F_1} \right) \\ \hat{c}_{12} + \hat{c}_{13} &= 2 + 2\gamma^{-1} \cos \left(S_1^J + \delta_3^J \frac{x-1}{\gamma F_1} \right). \end{aligned} \quad (49)$$

Plugging these in $S_3'^J$ expression yields

$$S_3'^J = \frac{\delta_3^J}{F_1} \frac{\kappa \cos \left(\frac{S_3^B}{\kappa\gamma} + \frac{\delta_3^J(x-1)}{\gamma F_1} + \alpha \right) - \gamma}{\kappa\gamma - \cos \left(\frac{S_3^B}{\kappa\gamma} + \frac{\delta_3^J(x-1)}{\gamma F_1} + \alpha \right)}. \quad (50)$$

The details of the loops zipping, unzipping and disentanglement were studied in [19]. Here we briefly outline the main results. For the junctions to form one requires that $0 < \alpha < \alpha_c$ where $\alpha_c = \arccos(\gamma/\kappa)$. The unzipping times for junctions B and D, x_D^u and x_B^u , satisfy

$$x_D^u - x_B^u = 2\gamma\alpha F_1 (1 - \kappa^{-2})^{-1} \left[1 - \frac{1}{\kappa\gamma} \frac{\sin \alpha}{\alpha} \right]. \quad (51)$$

Since $\sin \alpha/\alpha$ and $1/\kappa\gamma$ are always less than unity, one concludes that $x_D^u > x_B^u$, indicating that the junction B which holds the external large arcs unzip sooner than the junction D

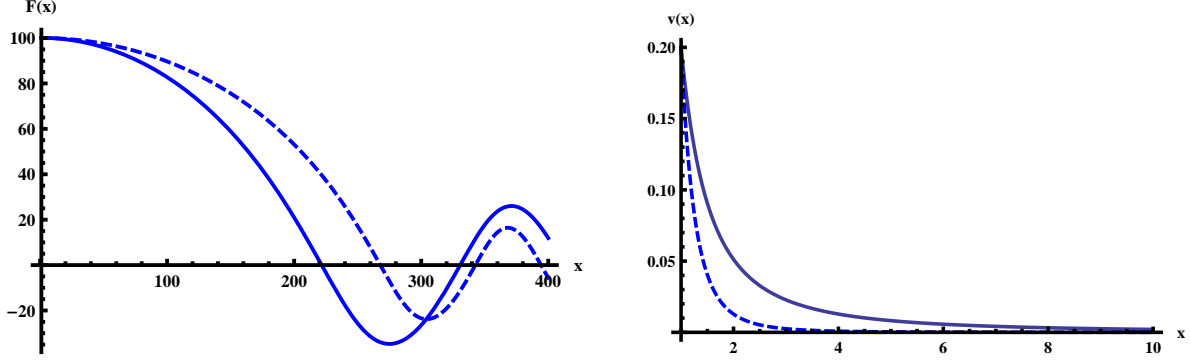


FIG. 2: Here the background evolution of Eqs. (30) and (31) are presented with $F_1 = 100, v_1 = 0.2$ and $F'(x = 1) = 0.1$. The left figure shows $F(x)$ whereas the right figure represents $v(x)$. The solid lines are for the radiation dominated backgrounds ($n = 1$) and the dashed lines are for the matter dominated backgrounds ($n = 2$). We are considering the loops evolution until they shrink, i.e. until the first root of $F(x) = 0$.

which holds the internal smaller arcs. Although we have proved this only for small sub-horizon loops but our numerical analysis show that this conclusion holds true in general.

The loops disentangle at the time x_f when $S_3 = 0$, which is given by the parametric relation

$$\kappa\gamma \cos^{-1} \Gamma - \cos\left(\frac{x_f - 1}{\gamma F_1}\right) \sqrt{1 - \Gamma^2} - \kappa\gamma \mu_1 \alpha + \sin \alpha = 0, \quad (52)$$

where

$$\Gamma \equiv \left[\frac{(x_f - 1)}{\kappa F_1 \sin(\frac{x_f - 1}{\gamma F_1})} \right].$$

This is an implicit equation for x_f which should be solved in terms of κ, γ, α and F_1 . For this to make sense, we demand that $x_f - 1 < \gamma F_1 \pi/2$ before the loops shrink to zero.

IV. NUMERICAL ANALYSIS

In this section we present our full numerical results for different loops configurations. To be specific, we consider three examples of (a): large super-horizon size loops with $F_1 = 100$, (b): intermediate size loops with $F_1 = 0.5$ and (c): small sub-horizon size loops with $F_1 = 0.01$.

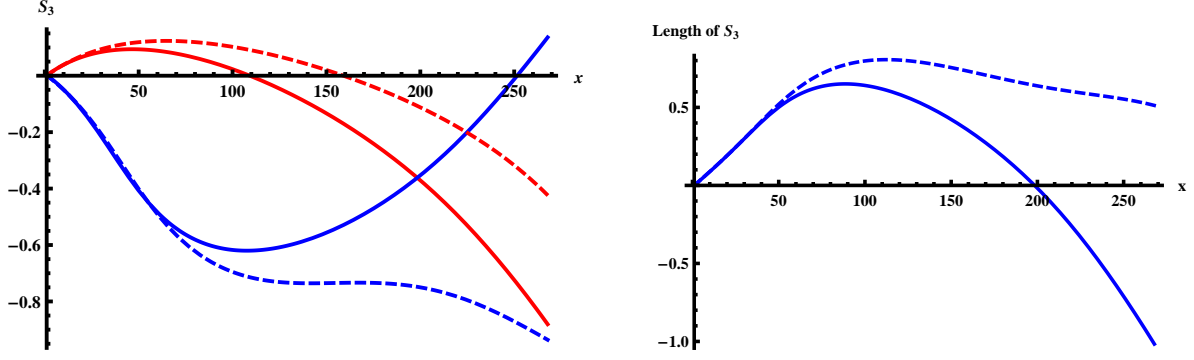


FIG. 3: In these plots we have presented the evolution of junctions B and D for $F_1 = 100$, $\alpha = \pi/9$ and $\kappa = 1.2$. In the left figure the upper solid red curve represents S_3^B whereas the lower solid blue curve is that of S_3^D for the radiation dominated background. The dashed curve represents the corresponding curves in the matter dominated background. The right graph represents the length of the newly formed strings μ_3 , $S_3 \equiv S_3^B - S_3^D$. The solid (dashed) curve is for the radiation (matter) dominated background. We see that in both backgrounds, after junction formation, the string BD reaches a maximum length and get unzipped. However, only in the radiation dominated background S_3 becomes zero before loops shrink indicating the loops disentanglement.

A. Large super-horizon size loops

For super-horizon size loops with $F_1 \gg 1$ one expects that the loops are conformally stretched until they re-enter the horizon. In this period, the loops lose much of its center of mass velocity as demonstrated by Eq. (43). As mentioned before, the loss of velocity is more significant for the matter dominated backgrounds. Also from Eq. (42) we see that it takes longer for the loop to shrink for the matter dominated backgrounds as compared to the radiation dominated backgrounds. Both of these analytical conclusions were verified in our full numerical investigations. In **Fig.2** we have presented the background solutions of $F(x)$ and $v(x)$ solving Eqs. (30) and (31) numerically. As is clear from the figure, in a matter dominated background, it takes longer for the loop to shrink. This in turn plays some roles in the junctions evolutions and loops disentanglement. In **Fig.3** we have presented the evolutions of junction B and D solving Eq. (39) numerically. The left figure shows the evolution of junctions B and D both for matter and radiation dominated backgrounds. The

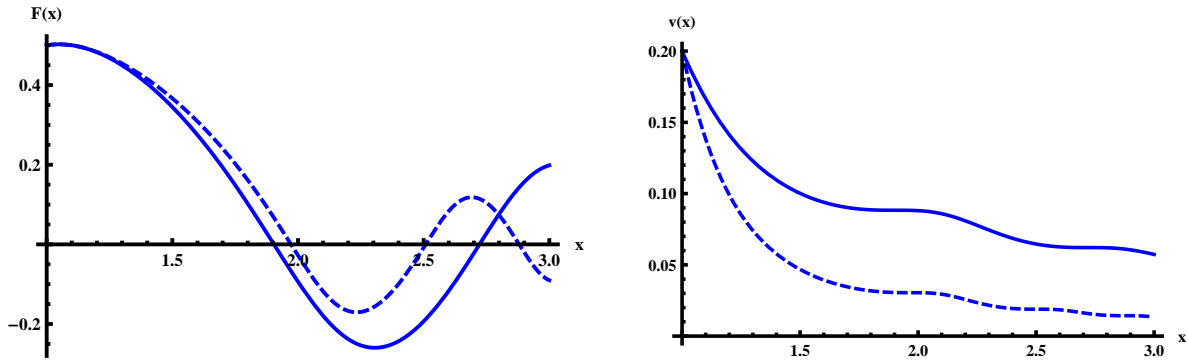


FIG. 4: Here the background evolution for $F(x)$ and $v(x)$ are presented with $F_1 = 0.5, v_1 = 0.2, F'(x = 1) = 0.1$. The solid (dashed) curves are for the radiation (matter) dominated backgrounds.

right figure shows the length of the newly formed string μ_3 stretching between junctions B and D which is $S_3 \equiv S_3^B - S_3^D$. As mentioned previously for the junction to form we require that $S_3' > 0$. From the right figure we see that the junction is created in both cosmological backgrounds. After the junction formation, S_3 reaches a maximum value indicating the unzipping of the newly formed strings BD . After this time, S_3 reduces. When $S_3 = 0$ the junctions B and D meet again and the loops disentangle and pass by from each other. From the right figure we see that for the radiation dominated background the loops disentanglement indeed take place. However, for the matter dominated background, we see that before loops find the opportunity to disentangle, they shrink to zero. As explained below Eq. (51) the junction B unzips sooner than junction D which is also demonstrated in the left figure of **Fig. 3**.

B. Loops with intermediate sizes

For the loops with the sizes comparable to the Hubble radius at the time of collision, $F_1 \sim 1$, we can only do numerical analysis. On the physical grounds one expects that the evolution of $F(x)$ and $v(x)$ is less sensitive to the background cosmological expansion as compared to large super-horizon size loops. In **Fig. 4** we have presented the background evolution of $F(x)$ and $v(x)$ for $F_1 = 0.5$. As expected $v(x)$ changes slowly and $F(x)$ evolves similarly for both matter and radiation dominated backgrounds. In **Fig. 5** we have presented

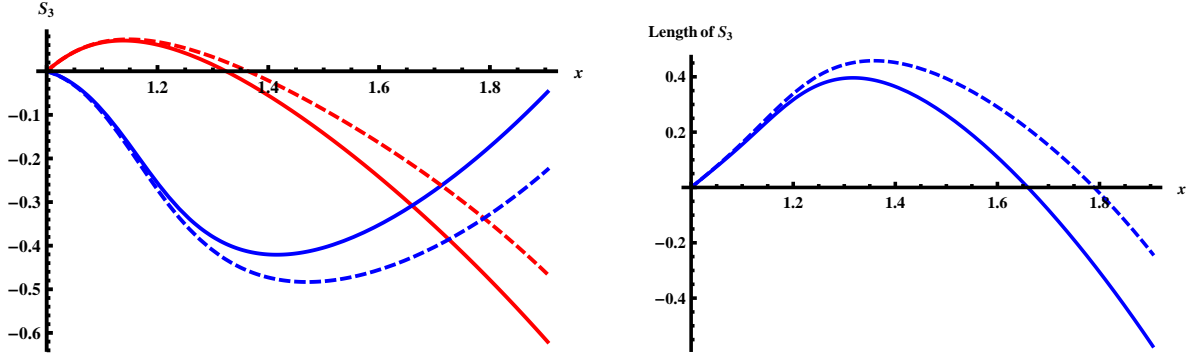


FIG. 5: Here we present the evolutions of junctions B and D and the string BD for $F_1 = 0.5$, $\alpha = \pi/9$ and $\kappa = 1.2$. In the left figure the upper solid red curve represents S_3^B whereas the lower solid blue curve is that of S_3^D for the radiation dominated background. The dashed curves represent the corresponding curves in the matter dominated background. The right graph represents the length of the newly formed string BD , S_3 . The solid (dashed) curve is for the radiation (matter) dominated background. We see that in both backgrounds, after junction formation, the string BD reaches a maximum length and get unzipped. We also observe that the onsets of string BD unzipping and the loops disentanglement happen sooner in a radiation dominated era.

the evolutions of junctions B , D and the string BD . For both radiation dominated and matter dominated backgrounds we see that the junctions are formed followed by the string BD unzipping and the loops disentanglement. One observes that the onsets of string BD unzipping (when S_3 reaches a maximum) and also the loops disentanglement happen earlier for the radiation dominated era as compared to the matter dominated era. This may be interpreted by noting that for the radiation dominated backgrounds the loops reenter the horizon and shrink sooner as can be seen qualitatively from Eq. (42).

C. Small sub-horizon size loops

For small loops, $F_1 \ll 1$, as explained before one expects the background cosmological evolutions do not play important roles. We have presented the analytical results for small loops in subsection III B. In **Fig. 6** we have presented the full numerical solutions of $F(x)$ and $v(x)$. As expected $F(x)$ shows simple periodic behavior and $v(x)$ does not change much

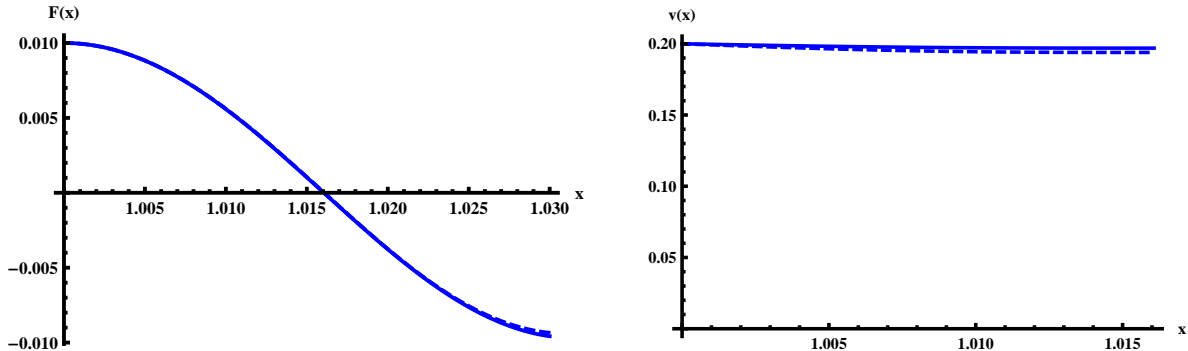


FIG. 6: Here the solutions of $F(x)$ and $v(x)$ for both matter dominated and radiation dominated backgrounds are shown for $F_1 = 0.01, v_1 = 0.2$ and $F'(x = 1) = 0$. As expected, the background cosmological evolutions do not play important roles so $F(x)$ indicates simple periodic behavior and $v(x)$ changes slowly.

in each period. In **Fig. 7** we have presented the junctions evolution. As expected, the junctions evolutions are identical for both matter and radiation dominated backgrounds. We also observe that the string BD unzipping and the loops disentanglement take place in this example. As demonstrated analytically in Eq. (51) the junction B unzips sooner than junction D which is also demonstrated in the left figure of **Fig. 7**.

V. CONCLUSION

In this work we have studied the cosmic strings collision in cosmological backgrounds. After presenting the general formalism in section II we have concentrated to the example of colliding loops. The motivation for this work was to understand analytically the findings of simulation in [20] where it was found that there were little contributions from the bound states strings in their multiple strings network. One can understand this phenomena as follows. For the junctions to develop upon strings collision, some appropriate initial conditions should be satisfied. These depends on the relative tensions of the colliding strings, the angle of collision and their relative velocities. Yet the more interesting observation is that even when junctions are created, they can not grow indefinitely and the bound state strings start to unzip.

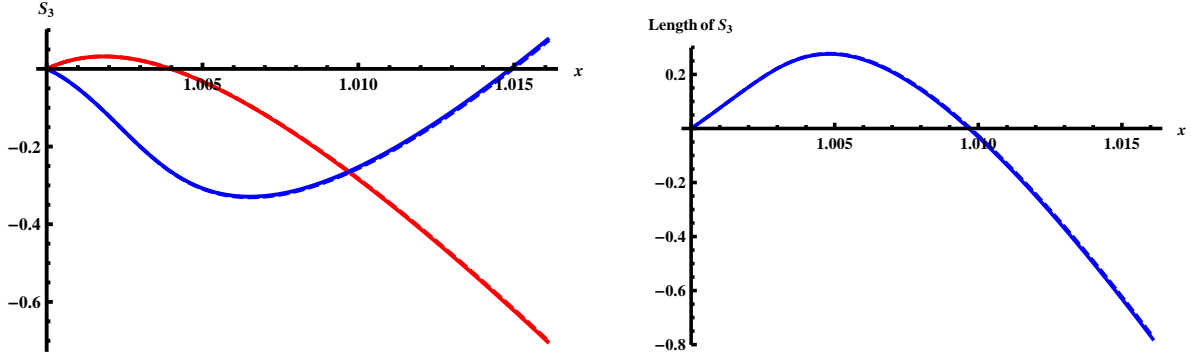


FIG. 7: Here the junctions evolutions are shown for $F_1 = 0.01$, $\alpha = \pi/9$ and $\kappa = 1.2$. In the left figure, the upper red (lower blue) curve shows S_3^B (S_3^D). Interestingly the curves corresponding to the radiation and the matter dominated backgrounds coincide to each other. As demonstrated by Eq. (51) the junction B unzip sooner than the junction D . The right figure shows the length of string BD given by S_3 . Again the curves corresponding to the matter dominated and the radiation dominated backgrounds coincide.

As described in [19], for straight cosmic strings at collision the junctions do not unzip once they are materialized. However, for colliding loops in a flat background the zipping and unzipping generically happen [19]. The natural question is how sensitive are these results to the expansion of the Universe. Here we find some interesting results indicating that the background expansion plays important roles in strings zipping, unzipping and their eventual disentanglement. The key parameter here is the relative size of the loops compared to the Hubble expansion rate at the time of collision. For large super-horizon size loops one may approximate them with straight strings. This implies that if junctions are formed upon loops collision it will grow initially as in straight strings examples. However, as the Universe expands the loops stretch conformally until they re-enter the Horizon. Meanwhile their velocities reduces rapidly. The net effect is that the rate of bound state strings creation slows down until it starts to unzip. Eventually the loops disentangle from each other and pass by from each other in opposite directions if they did not shrink to zero by then. On the other hand, for small sub-horizon size loops one can neglect the effects of the expansion and the results of [19] holds true. The case of colliding loops with the sizes comparable to the Hubble radius at the time of collision is more non-trivial which shares some features with

small and large loops cases.

Our numerical investigations also show that the junction formation and the zipping and unzipping phenomena are sensitive to the angle of collision α and the strings relative tensions parametrized by κ . It would be interesting to study these phenomena in the multi parameter space of F_1, κ and α . Also to simplify the analysis, we have restricted ourselves to the example of coplanar colliding loops with equal tensions and radii. It would be interesting to study the general case where the loops have different sizes and orientations and there are hierarchies between the sizes of the loops and the Hubble expansion rate at the time of collision.

Acknowledgments

We would like to thank Tom Kibble for useful discussions and comments.

References

-
- [1] S. Sarangi and S. H. H. Tye, “Cosmic string production towards the end of brane inflation,” *Phys. Lett. B* **536**, 185 (2002) [arXiv:hep-th/0204074].
 - [2] M. Majumdar and A. Christine-Davis, “Cosmological creation of D-branes and anti-D-branes,” *JHEP* **0203**, 056 (2002) [arXiv:hep-th/0202148].
 - [3] E. J. Copeland and T. W. B. Kibble, “Cosmic Strings and Superstrings,” *Proc. Roy. Soc. Lond. A* **466**, 623 (2010) [arXiv:0911.1345 [hep-th]].
 - [4] S. H. Henry Tye, “Brane inflation: String theory viewed from the cosmos,” *Lect. Notes Phys.* **737**, 949 (2008) [arXiv:hep-th/0610221].
 - [5] T. W. B. Kibble, “Cosmic strings reborn?,” *astro-ph/0410073*.
 - [6] A. C. Davis and T. W. B. Kibble, “Fundamental cosmic strings,” *Contemp. Phys.* **46**, 313 (2005) [arXiv:hep-th/0505050].
 - [7] M. Sakellariadou, “Cosmic Superstrings,” *arXiv:0802.3379 [hep-th]*.
 - [8] B. Shlaer and M. Wyman, “Cosmic superstring gravitational lensing phenomena: Predictions for networks of (p,q) strings,” *Phys. Rev. D* **72**, 123504 (2005) [arXiv:hep-th/0509177].

- [9] R. Brandenberger, H. Firouzjahi and J. Karouby, “Lensing and CMB Anisotropies by Cosmic Strings at a Junction,” *Phys. Rev. D* **77**, 083502 (2008) [arXiv:0710.1636 [hep-th]];
T. Suyama, “Exact gravitational lensing by cosmic strings with junctions,” *Phys. Rev. D* **78**, 043532 (2008) [arXiv:0807.4355 [astro-ph]].
- [10] R. Brandenberger, H. Firouzjahi, J. Karouby and S. Khosravi, “Gravitational Radiation by Cosmic Strings in a Junction,” *JCAP* **0901**, 008 (2009) [arXiv:0810.4521 [hep-th]];
M. G. Jackson and X. Siemens, “Gravitational Wave Bursts from Cosmic Superstring Reconnections,” *JHEP* **0906**, 089 (2009) [arXiv:0901.0867 [hep-th]];
P. Binetruy, A. Bohe, T. Hertog and D.A. Steer, “Gravitational Wave Bursts from Cosmic Superstrings with Y-junctions,” arXiv:0907.4522.
- [11] L. Leblond, B. Shlaer and X. Siemens, “Gravitational Waves from Broken Cosmic Strings: The Bursts and the Beads,” arXiv:0903.4686 [astro-ph.CO].
- [12] E. J. Copeland, R. C. Myers and J. Polchinski, “Cosmic F- and D-strings,” *JHEP* **0406**, 013 (2004), hep-th/0312067 ;
G. Dvali and A. Vilenkin, “Formation and evolution of cosmic D-strings,” *JCAP* **0403**, 010 (2004) [arXiv:hep-th/0312007];
L. Leblond and S.-H. H. Tye, “Stability of D1-strings inside a D3-brane,” *JHEP* **0403**, 055 (2004), hep-th/0402072;
N. Barnaby, A. Berndsen, J. M. Cline and H. Stoica, “Overproduction of cosmic superstrings,” *JHEP* **0506**, 075 (2005) [arXiv:hep-th/0412095].
- [13] H. Firouzjahi, L. Leblond and S. H. Henry Tye, “The (p,q) string tension in a warped deformed conifold,” *JHEP* **0605**, 047 (2006) hep-th/0603161;
H. Firouzjahi, “Dielectric (p,q) strings in a throat,” *JHEP* **0612**, 031 (2006) hep-th/0610130;
K. Dasgupta, H. Firouzjahi and R. Gwyn, “Lumps in the throat,” *JHEP* **0704**, 093 (2007) [arXiv:hep-th/0702193];
M. Lake, S. Thomas and J. Ward, “String Necklaces and Primordial Black Holes from Type IIB Strings,” arXiv:0906.3695 [hep-ph].
- [14] M. G. Jackson, N. T. Jones and J. Polchinski, “Collisions of cosmic F- and D-strings,” *JHEP* **0510**, 013 (2005), hep-th/0405229;
A. Hanany and K. Hashimoto, “Reconnection of colliding cosmic strings,” *JHEP* **0506**, 021 (2005) [arXiv:hep-th/0501031];

- K. Hashimoto and D. Tong, “Reconnection of non-abelian cosmic strings,” JCAP **0509**, 004 (2005) [arXiv:hep-th/0506022];
- M. Eto, K. Hashimoto, G. Marmorini, M. Nitta, K. Ohashi and W. Vinci, “Universal reconnection of non-Abelian cosmic strings,” Phys. Rev. Lett. **98**, 091602 (2007) [arXiv:hep-th/0609214];
- M. G. Jackson, “Interactions of cosmic superstrings,” JHEP **0709**, 035 (2007) [arXiv:0706.1264 [hep-th]].
- [15] H. Firouzjahi, “Energy Radiation by Cosmic Superstrings in Brane Inflation,” Phys. Rev. D **77**, 023532 (2008) [arXiv:0710.4609 [hep-th]].
- [16] Y. Cui, S. P. Martin, D. E. Morrissey and J. D. Wells, “Cosmic Strings from Supersymmetric Flat Directions,” Phys. Rev. D **77**, 043528 (2008) [arXiv:0709.0950 [hep-ph]].
- [17] A. C. Davis, W. Nelson, S. Rajamanoharan and M. Sakellariadou, “Cusps on cosmic superstrings with junctions,” arXiv:0809.2263 [hep-th].
- [18] S. H. Tye, I. Wasserman and M. Wyman, “Scaling of multi-tension cosmic superstring networks,” Phys. Rev. D **71**, 103508 (2005) [Erratum-ibid. D **71**, 129906 (2005)] [arXiv:astro-ph/0503506];
- L. Leblond and M. Wyman, “Cosmic necklaces from string theory,” astro-ph/0701427;
- A. Avgoustidis and E. P. S. Shellard, “Velocity-Dependent Models for Non-Abelian/Entangled String Networks,” arXiv:0705.3395 [astro-ph];
- A. Rajantie, M. Sakellariadou and H. Stoica, “Numerical experiments with p F- and q D-strings: the formation of (p,q) bound states,” arXiv:0706.3662 [hep-th];
- M. Sakellariadou and H. Stoica, “Dynamics of F/D networks: the role of bound states,” JCAP **0808**, 038 (2008) [arXiv:0806.3219 [hep-th]].
- [19] H. Firouzjahi, J. Karouby, S. Khosravi and R. Brandenberger, “Zipping and Unzipping of Cosmic String Loops in Collision,” Phys. Rev. D **80**, 083508 (2009) [arXiv:0907.4986 [hep-th]].
- [20] J. Urrestilla and A. Vilenkin, “Evolution of cosmic superstring networks: a numerical simulation,” JHEP **0802**, 037 (2008) [arXiv:0712.1146 [hep-th]].
- [21] L. M. A. Bettencourt and T. W. B. Kibble, “Nonintercommuting Configurations In The Collisions Of Type I U(1) Cosmic Strings,” Phys. Lett. B **332**, 297 (1994) [arXiv:hep-ph/9405221].
- [22] E. J. Copeland, T. W. B. Kibble and D. A. Steer, “Collisions of strings with Y junctions,”

- Phys. Rev. Lett. **97**, 021602 (2006) [arXiv:hep-th/0601153].
- [23] E. J. Copeland, T. W. B. Kibble and D. A. Steer, “Constraints on string networks with junctions,” Phys. Rev. D **75**, 065024 (2007) [arXiv:hep-th/0611243].
 - [24] E. J. Copeland, H. Firouzjahi, T. W. B. Kibble and D. A. Steer, “On the Collision of Cosmic Superstrings,” Phys. Rev. D **77**, 063521 (2008) [arXiv:0712.0808 [hep-th]].
 - [25] P. Salmi, A. Achúcarro, E. J. Copeland, T. W. B. Kibble, R. de Putter and D. A. Steer, “Kinematic Constraints on Formation of Bound States of Cosmic Strings - Field Theoretical Approach,” Phys. Rev. D **77**, 041701 (2008) [arXiv:0712.1204 [hep-th]].
 - [26] N. Bevis and P. M. Saffin, “Cosmic string Y-junctions: a comparison between field theoretic and Nambu-Goto dynamics,” Phys. Rev. D **78**, 023503 (2008) [arXiv:0804.0200 [hep-th]].
 - [27] A. Achúcarro and R. de Putter, “Effective non-intercommutation of local cosmic strings at high collision speeds,” Phys. Rev. D **74**, 121701 (2006) [arXiv:hep-th/0605084].
 - [28] N. Bevis, E. J. Copeland, P. Y. Martin, G. Niz, A. Pourtsidou, P. M. Saffin and D. A. Steer, “On the stability of Cosmic String Y-junctions,” arXiv:0904.2127 [hep-th].
 - [29] N. Turok and P. Bhattacharjee, “Stretching Cosmic Strings,” Phys. Rev. D **29**, 1557 (1984).